Available online at www.sciencedirect.com
ScienceDirect
Remote Sensing of Environment 112 (2008) 681–696
Remote Sensing of Environment
www.elsevier.com/locate/rse

Space-based detection of wetlands' surface water level changes from L-band SAR interferometry

Shimon Wdowinski [a,*], Sang-Wan Kim [a], Falk Amelung [a], Timothy H. Dixon [a], Fernando Miralles-Wilhelm [b], Roy Sonenshein [c]

[a] Division of Marine Geology and Geophysics, University of Miami, 4600 Rickenbacker Causeway, Miami, FL 33149-1098, United States
[b] Department of Civil, Architectural and Environmental Engineering, University of Miami, Coral Gables FL 33124, United States
[c] U.S. Geological Survey, Florida Integrated Science Center, 3110 SW 9th Avenue, Ft. Lauderdale, Florida 33315, United States

Received 9 February 2006; received in revised form 5 June 2007; accepted 7 June 2007

Abstract

Interferometric processing of JERS-1 L-band Synthetic Aperture Radar (SAR) data acquired over south Florida during 1993–1996 reveals detectable surface changes in the Everglades wetlands. Although our study is limited to south Florida it has implication for other large-scale wetlands, because south Florida wetlands have diverse vegetation types and both managed and natural flow environments. Our analysis reveals that interferometric coherence level is sensitive to wetland vegetation type and to the interferogram time span. Interferograms with time spans less than six months maintain phase observations for all wetland types, allowing characterization of water level changes in different wetland environments. The most noticeable changes occur between the managed and the natural flow wetlands. In the managed wetlands, fringes are organized, follow patterns related to some of the managed water control structures and have high fringe-rate. In the natural flow areas, fringes are irregular and have a low fringe-rate. The high fringe rate in managed areas reflects dynamic water topography caused by high flow rate due to gate operation. Although this organized fringe pattern is not characteristic of most large-scale wetlands, the high level of water level change enables accurate estimation of the wetland InSAR technique, which lies in the range of 5–10 cm. The irregular and low rate fringe pattern in the natural flow area reflects uninterrupted flow that diffuses water efficiently and evenly. Most of the interferograms in the natural flow area show an elongated fringe located along the transitional zone between salt- and fresh-water wetlands, reflecting water level changes due to ocean tides.

Keywords: Wetlands; Everglades; Surface flow; InSAR

1. Introduction

Interferometric Synthetic Aperture Radar (InSAR) is a powerful technique for detecting small changes (cm level resolution) of the Earth's surface over a wide area. The method is widely used to study earthquake and volcanic induced crustal deformation (e.g., Burgmann et al., 2000; Massonnet & Feigl, 1998; Massonnet et al., 1993), land subsidence (e.g., Amelung et al., 1999; Baer et al., 2002; Bawden et al., 2001; Buckley et al., 2003), landslides (e.g., Colesanti & Wasowski, 2006; Dai et al., 2002; Kimura & Yamaguchi, 2000), mining and large-scale geotechnical projects (e.g., Raucoules et al., 2003; Tesauro et al., 2000), and glacier motion (e.g., Goldstein et al., 1993; Mohr et al., 1998). The above applications measure the displacement of solid surfaces, whether they are rocks, soil, buildings, or ice (glacier). However, water level changes in wetlands may also be measured by InSAR (Alsdorf et al., 2000; Wdowinski et al., 2004a). This application works only in wetlands and floodplains where woody or herbaceous vegetation emerge above the water surface. The horizontal water surface and the vertical vegetation allow a double-bounce reflection of the transmitted radar signal back to the satellite (Richards et al., 1987). In non-vegetated flooded areas the water surface acts as a mirror scattering away the entire radar signal, because of the satellite's off-nadir transmission angle, typically 20°–45°.

* Corresponding author.
E-mail address: shimonw@rsmas.miami.edu. (S. Wdowinski).

0034-4257/$ - see front matter © 2007 Elsevier Inc. All rights reserved.
doi:10.1016/j.rse.2007.06.008

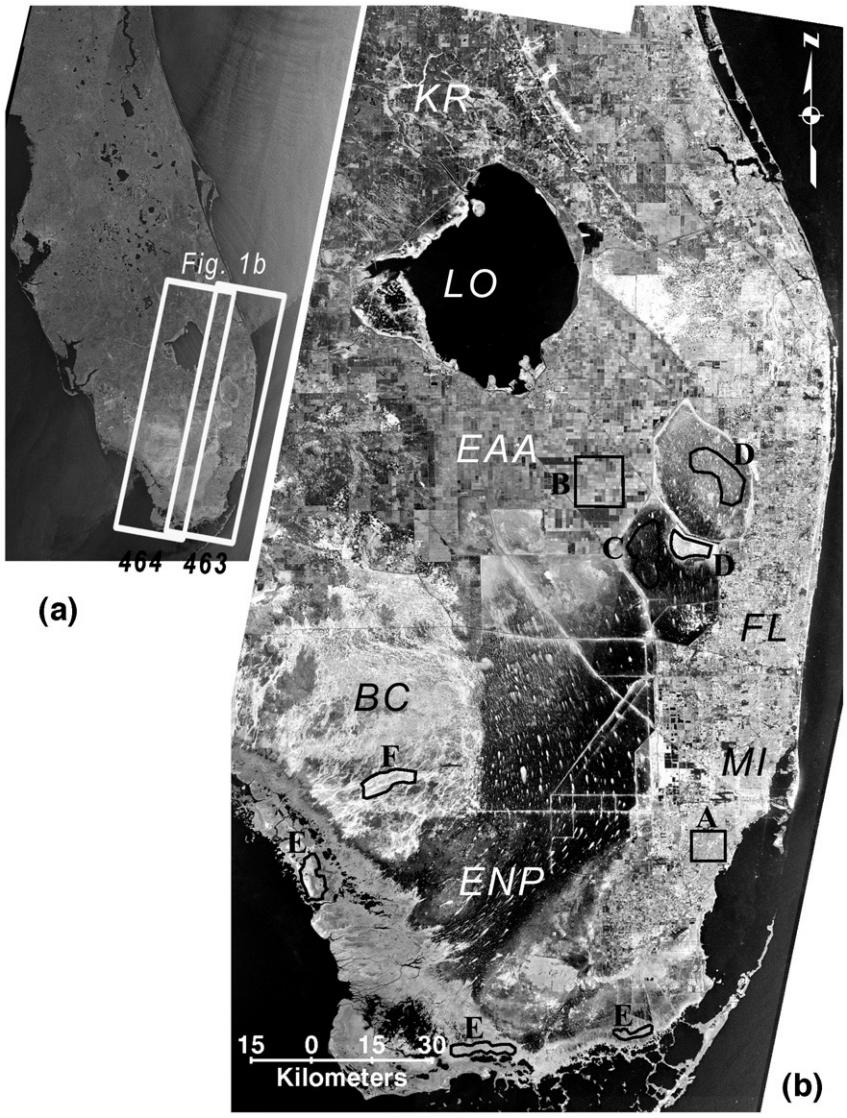

Fig. 1. (a) RADARSAT-1 ScanSAR image of Florida showing location of study area with two JERS-1 tracks' ground swath (RADARSAT data © Canadian Space Agency / Agence spatiale canadienne 2002. Processed by CSTARS and distributed by RADARSAT International). (b) JERS-1 L-band mosaic multi-temporal mean image of eastern and central south Florida. The study area includes: urban area along the coast (MI-FL), agricultural land south of Lake Okeechobee (EAA), and wetlands in between the agricultural area and the Gulf of Mexico (BC, and ENP). The wetland environment is divided into managed water conservation areas (in the central part of the image) and the remnant of the naturally flown Everglades in the southern part of the image. Both images show backscatter (brightness) variations, which depends on the surface dielectric properties and surface orientation with respect to the satellite. Areas marked by black frames and letters A–F are used to mark the backscatter and coherence studies presented in Table 1. Geographic locations: BC — Big Cypress National Preserve; EAA — Everglades Agricultural Area; ENP — Everglades National Park; FL — Fort Lauderdale; KR — Kissimmee River; and MI — Miami.

Space-borne SAR data have been acquired since the 1970's by several civilian satellites operating in the C- and L-band ranges (5.3 and 1.275 GHz corresponding to 5.66 and 23.5 cm wavelength, respectively). The longer wavelength L-band SAR data (23.5 cm wavelength) is considered more reliable for the InSAR technique in vegetated areas (Rosen et al., 1996; Zebker et al., 1997). The first applications of the InSAR method to floodplains and wetlands were conducted using L-band data acquired over the Amazon basin (Alsdorf et al., 2000) and southern Florida's Everglades wetlands (Wdowinski et al., 2004a). Recent studies have shown that the shorter wavelength C-band SAR data (5.66 cm) can also be used for wetland InSAR, mainly in woody wetland environment (Kim et al., 2005; Lu et al., 2005; Wdowinski et al., 2004a,b).

In this study, we use L-band SAR data to study water level changes and the derived hydrological conditions in the Everglades wetlands. The data were acquired over southern Florida during the years 1993–1996 by the Japanese Earth Resources Satellite (JERS-1). It is the most complete L-band dataset over a large-scale wetland acquired to date, containing seven repeat passes of two tracks that cover most of the Everglades wetlands. Because the Everglades consists of natural and managed wetland portions, as well as diverse vegetation types (woody, herbaceous, prairie, and saltwater mangroves), this large JERS-

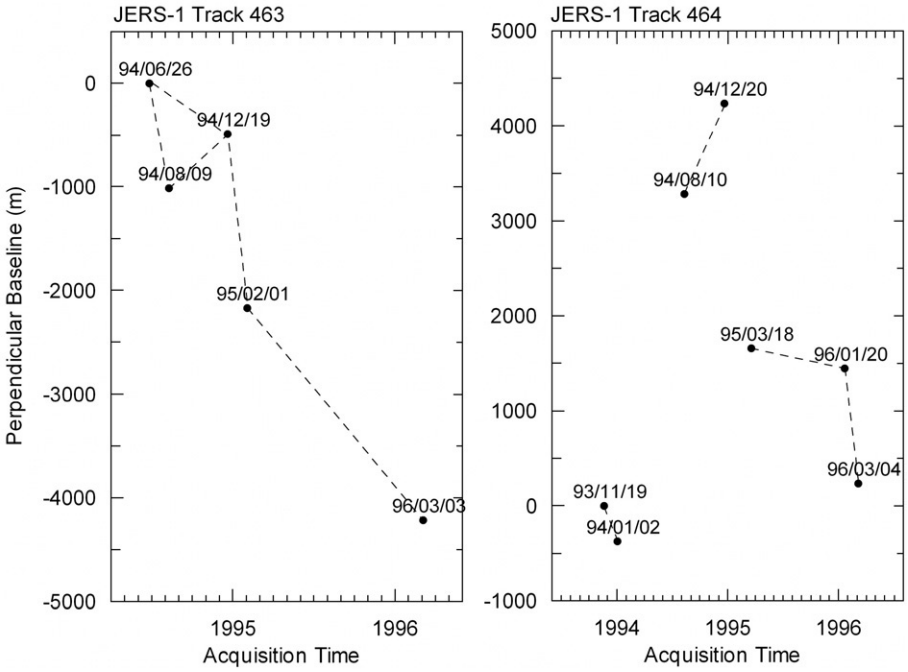

Fig. 2. Perpendicular baseline information with respect to the first acquisition of each JERS-1 tracks. Dotted line represents interferometric pair used in this study.

1 dataset allows a rigorous evaluation of the wetland InSAR method to various wetland environments.

In our previous study (Wdowinski et al., 2004a), we used three JERS-1 passes of one track acquired over six month period in second half of 1994. Here we expand this work in both spatial and temporal coverage. Our 2004 study focused on a limited region, specifically the Water Conservation Areas (WCA) located south of Lake Okeechobee (Fig. 1), where water level changes are largest and are dominated by the operation of human-made water control structures. In the current study, we use a more complete dataset (two tracks with seven repeat orbits) extending over a three year period. We also study a larger area, the entire south Florida wetlands, including both managed and natural flow wetland environments, as well as more diverse vegetation types. We find that the natural and managed flow environments have very different InSAR signatures, reflecting the different conditions in the two environments.

2. South Florida wetlands and hydrological background

South Florida is characterized by a large amount of precipitation (1200–1500 mm/yr) and very flat topography, resulting in a large volume of surface water that slowly drains to the ocean, evaporates, or infiltrates into the subsurface. The natural undisturbed system of south Florida, which existed until the beginning of the 20th century, includes the watershed of the Kissimmee River, Lake Okeechobee, and the Everglades (Fig. 1b). The Kissimmee River drains precipitation and runoff north of Lake Okeechobee into the lake, which discharges excess water southward to the Gulf of Mexico by a wide shallow sheet flow known as the Everglades "the river of grass" (Douglas, 1947). Anthropogenic changes in the past century, mainly for water supply, agricultural development and flood control purposes, have disrupted natural water flow. The current Everglades watershed includes the Everglades Agricultural Area (EAA, in Fig. 1b), a large urban area along the eastern cost of south Florida consisting of Miami (MI) and Fort Lauderdale (FL) and many other municipalities, natural flow area in the Everglades National Park (ENP) and the Big Cypress Natural Preserve (BC), and a large managed area in between (Water Conservation Areas), which is dissected by many levees, canals and other water control structures (Fig. 1b). Water flow in south Florida is administrated through the South Florida Water Management District (SFWMD), which operate a series of water control structures to prevent flooding and regulate flow and recharge rates. As a result, surface water often accumulates in controlled areas in excess of natural background levels.

South Florida is currently monitored by a network of stage (water level), meteorological, hydrogeologic, and water quality control stations, providing daily average estimates of water

Table 1
Calculated backscattering coefficient and interferometric coherence in six characteristic environments throughout south Florida

Mark in Fig. 1	Environment	Backscatter Coefficient sigma naught (dB)	Coherence	
		Average	Average	Std. Div.
A	Urban	−6.2	0.37	0.05
B	Sugar cane	−7.9	0.25	0.01
C	Sawgrass	−13.2	0.27	0.02
D	Graminoid prairie-marsh	−6.8	0.30	0.03
E	Mangrove swamp	−7.0	0.32	0.06
F	Cypress	−5.1	0.42	0.07

The locations of the different environments (A–F) are shown in Fig. 1.

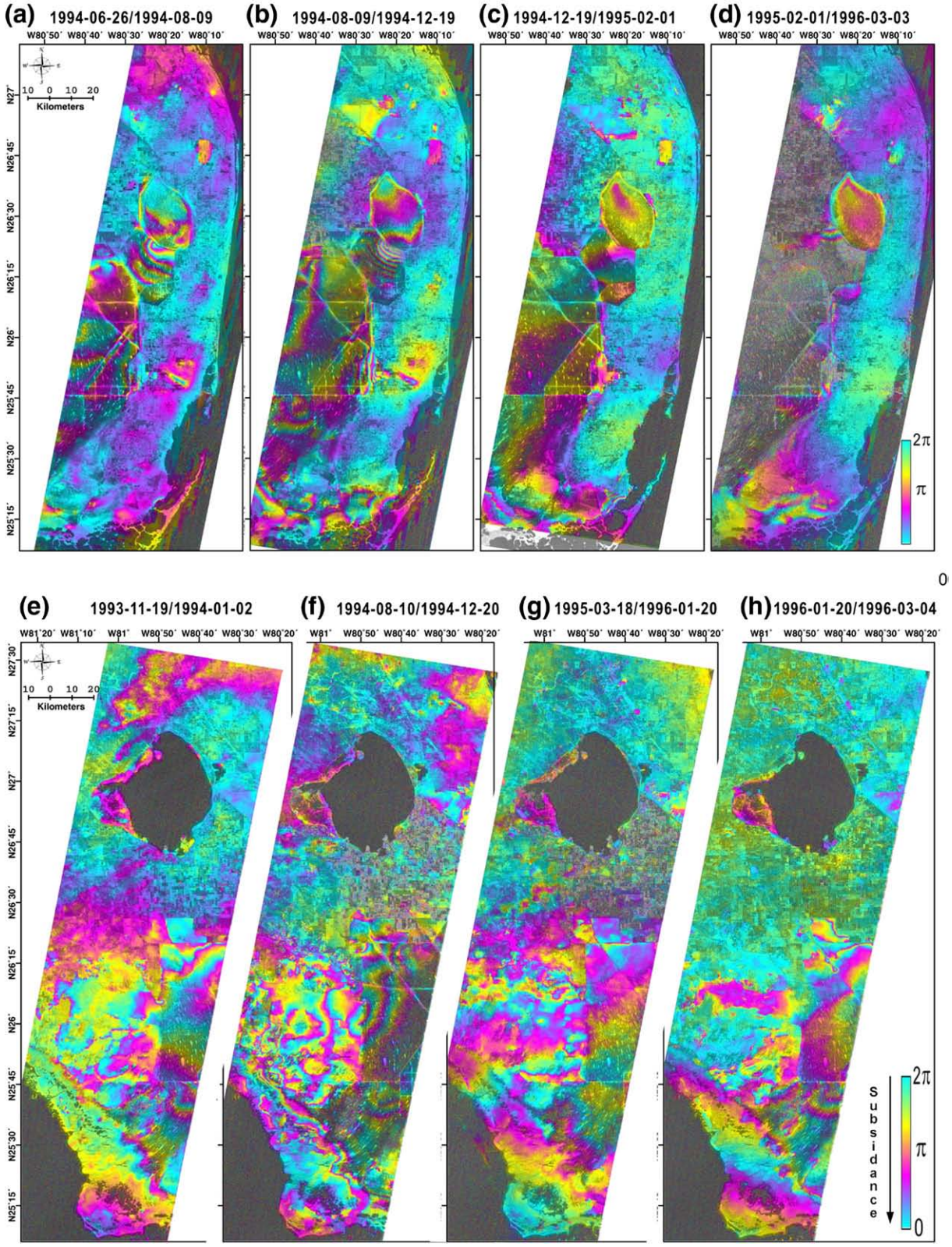

Fig. 3. Time series of JERS L-band interferograms showing phase changes in south Florida during 45–396 days. Upper panels show changes along the eastern track (463) and lower panels along the western track (464).

level, rainfall and other key hydrologic parameters. Due to operational and logistical reasons, most stage stations are located near water management structures and are typically spaced several kilometers apart. As a result, the interior of large water-covered areas, especially in the natural flow wetlands, are sparsely monitored. Space-based remote sensing observations

can provide high spatial resolution measurements of surface and hydrological conditions to augment the temporal resolution but lower spatial resolution ground based sensors. SAR observations are useful for such studies, because the radar signal is very sensitive to surface hydrological conditions. Previous SAR studies of south Florida focused on variations in radar backscatter to monitor changes in surface conditions (above ground biomass, soil moisture) and surface inundation during wet and dry seasons in southwestern Florida (Bourgeau-Chavez et al., 2005; Kasischke & Bourgeau-Chavez, 1997; Kasischke et al., 2003). Wdowinski et al. (2004a) used a different approach, employing SAR phase measurements with interferometric techniques (InSAR), for estimating centimeter-accuracy water level changes in the Everglades wetlands.

3. SAR data and InSAR processing

Our study is based on a large L-band SAR dataset acquired over south Florida during the years 1993–1996 by the JERS-1 satellite. The dataset includes twelve archived JERS-1 passes of two adjacent descending tracks; five repeat passes of the eastern track (463) and seven repeat passes of the western one (464) (Figs. 1a and 2). Although the data are archived and delivered by 75×75 km^2 scenes, we restored the original continuity of the data by concatenating the scenes, forming 225×75 km^2 continuous SAR coverage of eastern and central South Florida (Fig. 1).

Radar backscatter imagery from the JERS-1 L-band satellite can characterize the reflective properties of the Earth's surface and be used to identify wetlands, urbanized regions, and agriculture areas (Fig. 1b). The observed backscatter (brightness) variations depend on the scattering mechanism, surface dielectric properties, and surface orientation with respect to the satellite. The strongest backscatter contrast occurs in the wetland environment due to changes in the vegetation coverage and human-made structures. The most noticeable feature in both managed and natural wetlands are small, elongated high backscatter (white) areas, which are vegetated tree islands aligned along the long-term regional southward flow direction (Sklar et al., 2003). Another noticeable contrast occurs between the very bright Big Cypress Basin (BC in Fig. 1b) area and the darker Everglades, reflecting significant backscattering variations between the woody (BC) and herbaceous (Everglades) vegetations. A quantitative analysis of radiometrically calibrated backscattering intensity, which is conducted according to NASDA's user handbook (Shimada, 2002), in urban, agriculture, wetland environments (Table 1) shows that woody wetlands (e.g., cypress) and urban environments have the largest backscattering values, whereas herbaceous (e.g., sawgrass) wetlands have the lowest value.

We processed the concatenated JERS-1 data using the ROI_PAC software (Buckley et al., 2000). The interferogram calculations include phase unwrapping and topographic phase removal using the SRTM 1-arc second digital elevation model (DEM). When using short-intermediate baselines (<700 m), topographic phase removal is not necessary, because south Florida's very flat relief (< 5 m) contributes negligibly to phase changes. Based on the topography and baseline relation (Hanssen, 2001 — equation 1.2.12), a 700 m long baseline and 5 m topographic variation cause 0.05 cycle phase change, which is negligible with respect to the observed phase changes (1–7 cycles). However, when using longer baselines, as in some of our interferograms where baselines exceed 2000 m (Fig. 2), topographic phase removal should be considered. Unwrapped phase image with radar coordinate system was transformed to geographic coordinate system, using the lookup table obtained from the matching between Landsat ETM panchromatic orthorectified images of 15-m resolution (ftp.glcf.umiacs.umd.edu/glcf/Landsat/WRS2/) and radar backscatter imagery. In the post-processing stage, we applied adaptive radar interferogram filtering (Goldstein & Werner, 1998) and subsequent low-pass filtering to reduce noise and enhance fringe visibility. Although filtering improves the signal, it degrades the horizontal resolution, from 17 m to 100–300 m. The spatial resolution of the filtered

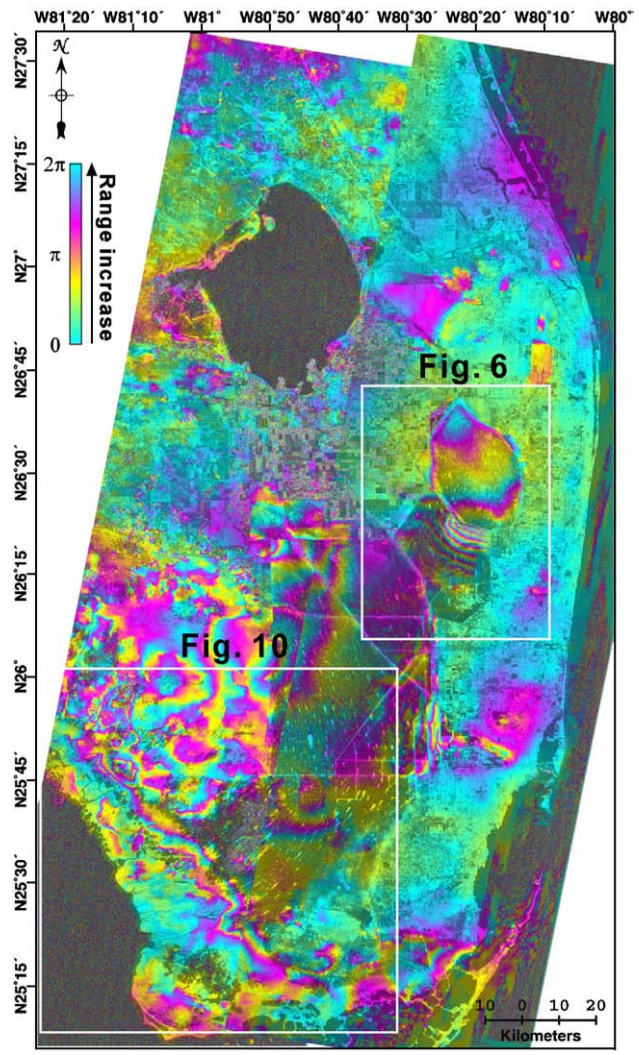

Fig. 4. Mosaic of JERS L-band interferograms of south Florida showing phase differences occurring during 135 days. The western track (464) covers the time span 1994/8/9–1994/12/19 and the eastern track (463) covers 1994/8/10–1994/12/20. The one day observation difference is reflected by some discontinuities along the track suture, only in the wetland area in the southern half of the image. Nevertheless, the small offsets along the suture suggest slow, but detectable, changes of water levels within a single day.

interferograms varies, because it is set dynamically by the adaptive filtering algorithm according to lateral noise distribution.

4. Results

We produced nine strip interferograms of south Florida showing phase changes between 44 and 396 days during the years 1993–1996 (dashed lines in Fig. 2). Eight of these are shown in Fig. 3, which includes interferograms of both the eastern track (upper panels) and the western track (lower panels). One interferogram (eastern track spanning over the period 1994-06-26/1994-12-19) is omitted, because of limited space of Fig. 3. It is of a similar quality and we refer to this interferogram in our analysis of the water managed areas (see below). Two of the interferograms (b and f), from the two different tracks, were calculated for almost the same time period. The eastern track (Fig. 3b) was acquired almost exactly one day prior to the western track (Fig. 3f), both in August and December, 1994. As the two interferograms also overlap one another by several kilometers, we found common phase features in both tracks that helped us combine the two interferograms and form a mosaic interferogram of most of south Florida (Fig. 4). The one day observation difference is reflected by some discontinuities along part of the track suture, mainly in the wetland areas. The significance of these discontinuities is discussed below.

The interferograms show good coherence throughout south Florida. Only the year-long interferogram (Fig. 3d) shows a significant area with no coherence, as coherence degrades with the interferogram time-span. Although coherence is maintained in all the shorter-term interferogram (44–176 days), it is not uniform. Coherence is higher in the woody wetlands and urban environments and lower in herbaceous wetlands and agricultural areas (Table 1). Interferometric coherence in south Florida as function of SAR wavelengths is addressed in a separate study (Kim et al., 2006).

The observed phase changes in both wetland and urban environments (Figs. 3 and 4) can be caused by surface displacement, atmospheric effects, and changes in surface dielectric properties. As discussed above, we applied topographic phase removal for longer baselines; hence topographic contribution to phase changes should be negligible. Similarly, a large change in dielectric properties throughout the study area seems unlikely; thus, we discard this possibility. Atmospheric changes, especially in tropical areas, can significantly affect the fringe pattern (Hanssen, 2001; Zebker et al., 1997). However, phase errors related to atmospheric water vapor are usually characterized by relatively short wavelength (kilometer-scale) spatial variations (Alsdorf et al., 2001; Zebker et al., 1997). Fig. 4 shows that most of the short wavelength lateral phase changes correlate with surface features, e.g., sharp or discontinuous changes across levees. Therefore, surface displacement is the most likely explanation for most of the observed phase changes.

Fringe patterns in wetlands environments reflect mostly vertical changes of water surfaces. In order to translate the measured phase changes along the radar line-of-sight, we need to correct the measurements for the incidence angle. For JERS-1 L-band observations (23.5 cm wavelength), each phase cycle (2π) corresponds to 11.75 cm of displacement in the radar line-of-sight. Taking into account the 39° satellite incidence angle, we obtain 15.1 cm vertical movement for each phase cycle (15.1 cm = half-wavelength / [cos(incidence angle)]), assuming

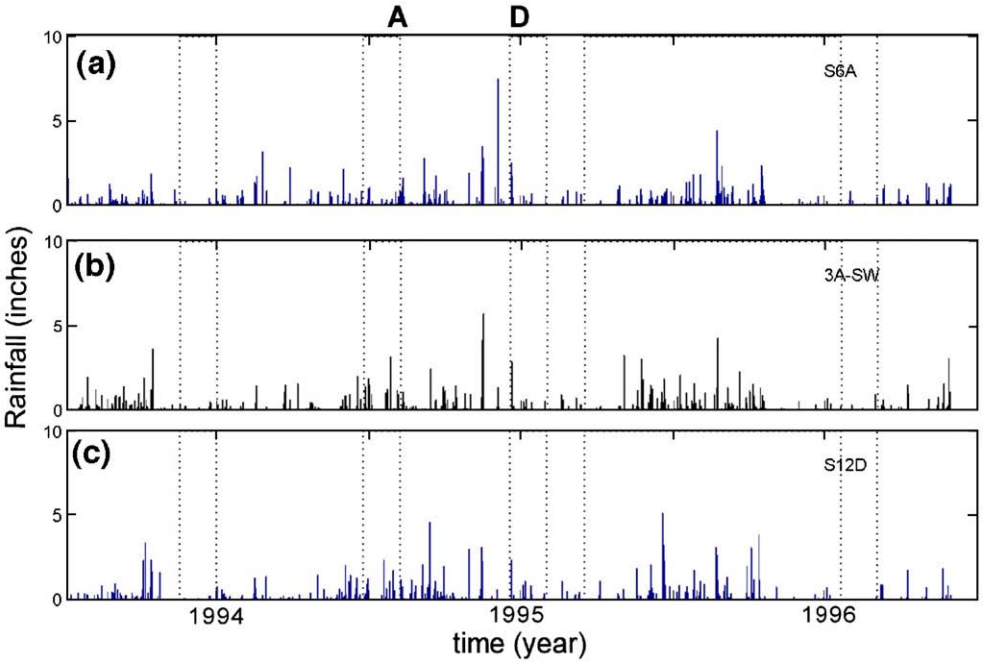

Fig. 5. Daily rainfall time series measured at 3 representative meteorological stations, located in the WCA-1 (a), southwestern part of WCA-3A (b), and in central part of the Tamiami Trail (c). The vertical dotted lines mark the JERS-1 acquisition dates. The data for the mosaic interferogram (Fig. 7) were acquired in August and December 1994 (marked by A and D, respectively), during severe rain events.

that all the displacement is vertical. Using the 15.1 cm value, it is possible to convert the unwrapped phase pattern to maps of surface level changes.

5. Hydrological analysis

The L-band interferograms presented here (Figs. 3 and 4) provide high spatial resolution (100–300 pixel resolution) maps of surface water level changes over broad wetland area. In order to utilize these space-based observations for hydrological application, we need additional information, because the InSAR measurements are relative in both time and space. In time, the measurements provide the change in water level (not the actual water level) that occurred between the data acquisitions (44–396 days). In space, the measurements describe the relative change of water levels in the entire interferogram with respect to a zero change at an arbitrary reference point, because the actual range between the satellite and the surface cannot be determined accurately. However the relative changes between pixels can be determined at the cm-level. In many other InSAR applications, such as earthquake or volcanic induced deformation, the reference zero change point is chosen to be in the far-field, where changes are known to be negligible (Massonnet et al., 1993). However in wetland InSAR, the assumption of zero surface change in the far-field does not hold, especially in the Everglades, because flow and water levels can be discontinuous across the various water control structures or other flow obstacles.

In order to utilize the high spatial resolution InSAR observations, we use stage (surface water elevation) and flow data to validate and calibrate the space-based observations. Fortunately, the Everglades wetlands are monitored by a dense network of stage, flow and meteorological stations. The data are archived at the SFWMD's DBHYDRO database (http://www.sfwmd.gov/org/ema/dbhydro/index.html), where the stage data are provided as daily average levels above the NGVD29 datum. The flow and the precipitation data are datum independent.

Based on the phase change patterns in the interferograms, we conducted two separated hydrological analyses, one of the WCAs and the other of the natural flow area. The eastern track interferograms (Fig. 3a–d) show organized (sub-parallel) and truncated fringes in the managed WCAs. The western track interferograms (Fig. 3e–h) show irregular fringe patterns in the

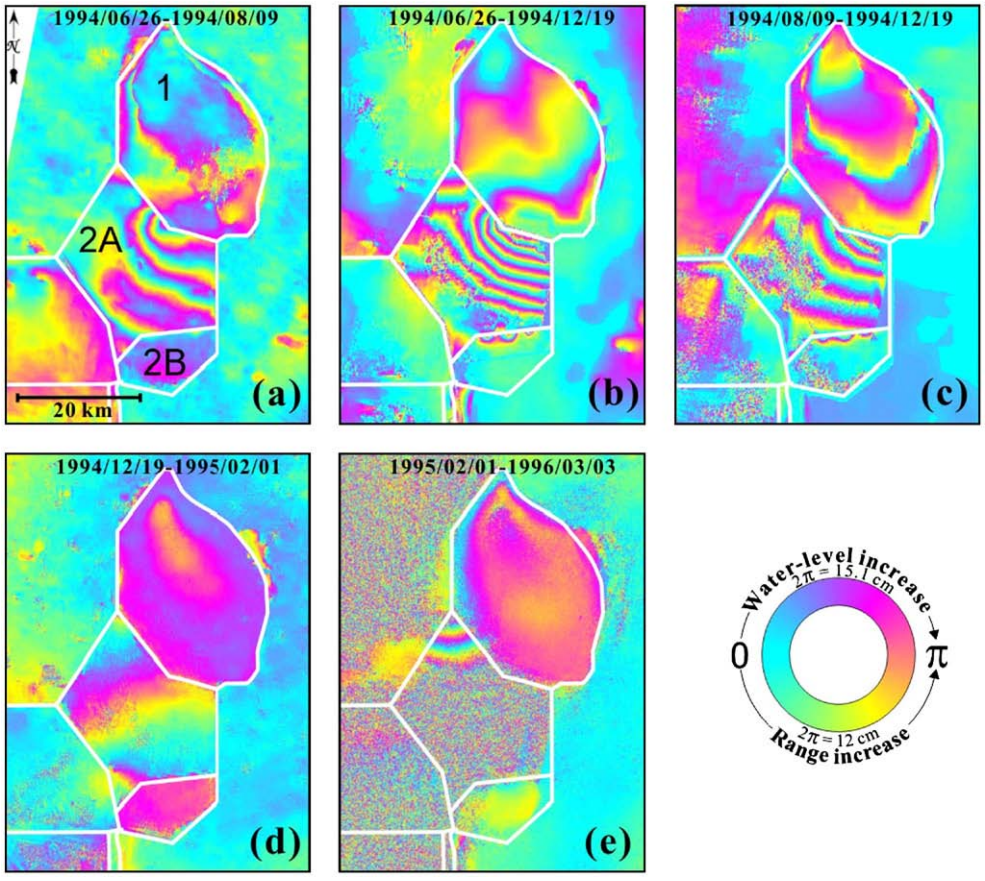

Fig. 6. Spatially filtered interferograms of the Water Conservation Areas (location in Figs. 1 and 4). (a) 44-day (June–August) interferogram (b) 176-day (June–December) interferogram, (c) 132-day (August–December) interferogram, (d) 44-day (December–February), and (e) 395-day (more than a year) interferogram. The interferograms show (i) the largest water level changes occurred in area 2A (up to 1 m — 7 cycles in (b)) and smaller scale ones in areas 1 and 2B. (ii) The pattern of water level change is unidirectional in the eastern section of area 2A and radial in the western part. In the northern section of area 2B the water level change is characterized by 3 bulls-eye radial patterns (b and c).

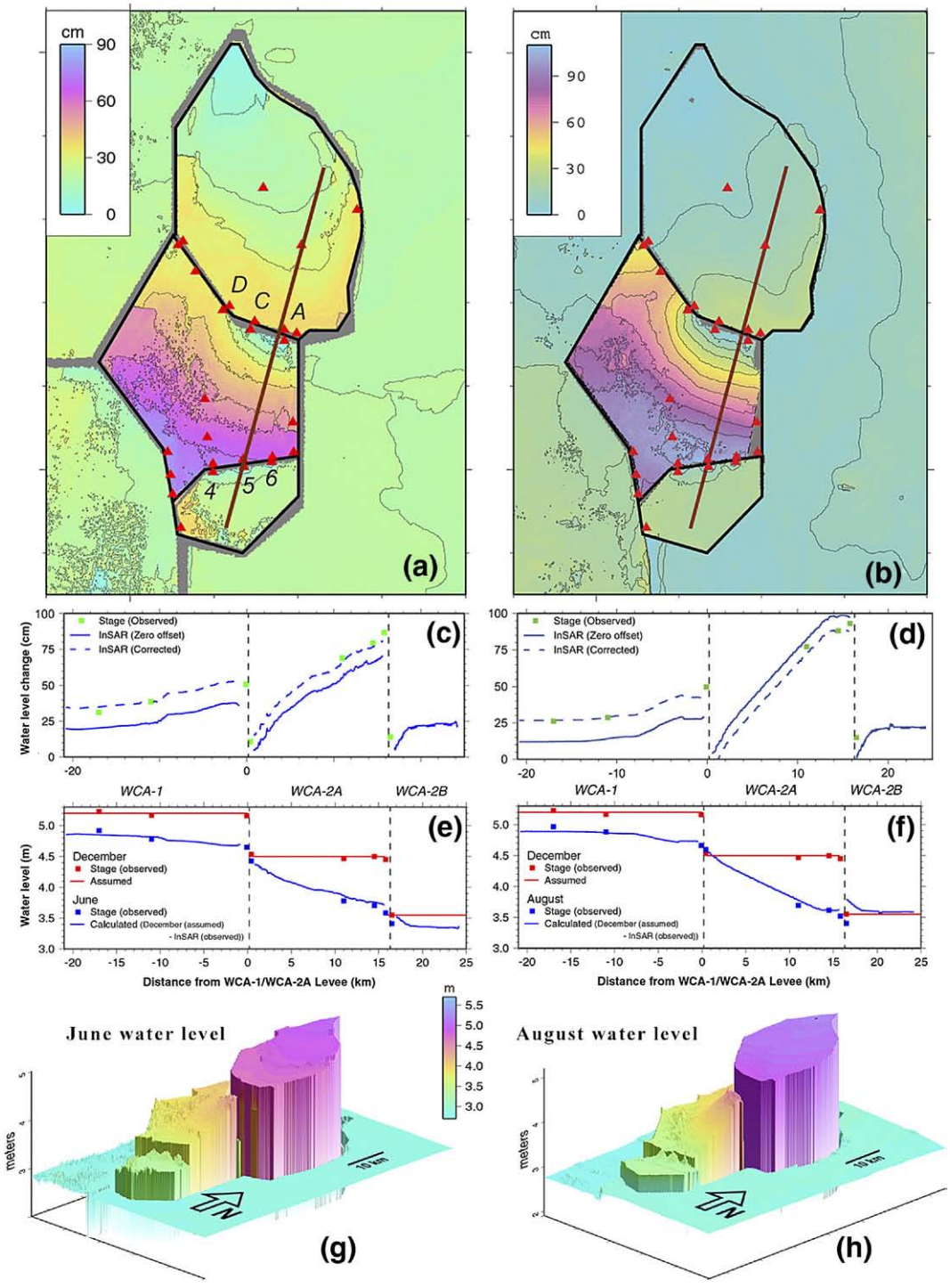

Fig. 7. (a and b) InSAR-based water level change maps of areas 1, 2A and 2B. Red triangles mark the location of stage stations and the brown line marks the water level profile location, which is drown perpendicular to water level contours. A, C, D, 4, 5, and 6 are gate locations (Table 2). (c and d) Comparison between InSAR and stage water level changes along the N–S profile. Stage data observed in the center of WCAs are projected onto the profile. The vertical dashed lines mark the location of levees separating between the WCAs. (e and f) Comparison between InSAR calculated levels (blue lines) and observed stage data for the June and August observations (blue squares). Our calculations assume flat water levels during the December SAR observation (red lines), which is justified by the December stage data (red squares) and the SFWMD flow data (Table 1). The calculated June and August curves are obtained by subtracting the observed InSAR data (blue lines in c and d) from the assumed December levels. (g and h) Three-dimensional illustrations of the June and August water levels, calculated by subtracting the corrected InSAR data from the assumed flat December levels.

southern section, mainly in the natural flow areas (ENP and BC). These different patterns are more apparent in the mosaic interferogram (Fig. 4), which contains more fringes than the other interferograms. We suspect that the high fringe rate in the mosaic interferogram reflects significant water level changes in the Everglades due to severe rainfall events occurring during both

the August and December acquisitions (Fig. 5). The hydrological analysis of the WCAs (upper box in Fig. 4) enables us to evaluate the accuracy of the InSAR wetland method due to the observed high fringe rate and a large number of ground-based stage stations located there. The analysis of the natural flow area (lower box) enables us to evaluate the application of the InSAR methods in natural undisturbed wetland environments.

5.1. Surface changes in the Water Conservation Areas

Here we focus on the northern section of the Everglades (upper box in Fig. 4), where the phase gradient is the highest and sufficient stage data is available to validate and calibrate the InSAR-based observations. We constructed a spatially filtered interferogram time-series of the WCAs (Fig. 6), showing phase changes occurring over time span of 44–396 days. Although each interferogram represents phase changes between different time periods, they share the following common characteristics: (i) Fringes are truncated along levees separating the WCAs; (ii) The largest water level changes occurred in area 2A (up to 1 m — 7 cycles in Fig. 6b); (iii) High fringe rates are found in the northern section of areas 2A and 2B (Fig. 6a, b, and c). The high fringe rate in area 2A extends over a wide area, and has a circular shape that is centered along the central and eastern section of the northern levee. The high fringe rate in area 2B shows three smaller radial ("bull's eye") patterns along the northern boundary of the area. The bull's eye patterns are centered about three culverts (gates) that allow flow from area 2A southward into area 2B. Two of the interferograms show only subtle phase changes (Fig. 6d and e) indicating little surface change.

We converted the unwrapped interferograms into maps of water level changes (Fig. 7a and b). This analysis differs somewhat from standard InSAR analysis because (1) water level changes across levees are discontinuous, and (2) there is no reference location with null displacement. To overcome these difficulties, we conducted the analysis separately for each of the areas and arbitrarily assigned zero value to the lowest change in each area. Thus, the maps in Fig. 7 show relative surface changes within each area, but not between areas. Although Fig. 6 shows that the largest changes occur in the southern part of area 2A, it is as likely that this area experienced less change than the northern section. If we set the southern region as our reference zero, we find that the largest change (with negative sign) occurs in the northern section of the study area. The important outcome of the analysis is not the absolute value of the water level change, but our ability to produce high spatial resolution maps (100–300 m pixel resolution) of surface water level changes within each area. In order to illustrate this point, we plot water level changes profiles across the three areas (Fig. 7c and d). The profile line is oriented perpendicular to water level contours in the eastern part of area 2A (brown lines in Fig. 7a and b). The profiles show that water level changes in each of the three areas are characterized by a southward increase. Because InSAR observations measure only relative change in water level, the assigned values are insignificant. However, the rate and shape of the curves are significant, because they represent the gradient and the spatial distribution of the water level change.

We compare the InSAR observations with stage data collected at 27 stations (red triangles in Figs. 7a and 8) to evaluate the accuracy of the InSAR method. The InSAR values are calculated from the nearest nine pixels to the stage station. Because most stage stations are located along levees and adjacent to flow gates (Fig. 7a and b), this comparison is not optimal. Stage data collected near flowing structures are affected by near-field flow dynamics (Lin & Gregg, 1988), which result in underestimation of stage near outflows and overestimation of stage near inflows. Similarly, due to our spatial filtering, the InSAR-based measurements of water level change reflect a wider area, up to several hundred meters in radius. Despite these possible biases, we compare between the zero-offset InSAR and the stage data, which are calculated separately for each area in each interferogram (Fig. 6). The comparison shows a good agreement between the two observation types, as indicated by the low root-mean-square (rms) deviation from the line with slope unity calculated using a least-squares method (Fig. 9). In the AUG–DEC and JUN–DEC interferograms, the calculated offset and rms in areas 2A and 2B (Fig. 9) are strongly influenced by 1–4 outliers (marked by circles). The outliers can represent either a problem with the InSAR observations or with the stage-related dynamic flow problem, as discussed above. The estimated rms with (12–15 cm) and with removed outliers (3–7 cm) are significantly different (Fig. 9). This suggests that the accuracy of the InSAR water level change measurements is 5–10 cm. The inferred precision is considerably better.

Another important result of the InSAR-stage comparison is the offset calculation (Fig. 9), which allows correction for the absolute water level changes within each of the areas. As indicated above, during the translation of phase changes to maps of water level changes, we defined arbitrarily the lowest change within each area as zero. The offset calculation provides us the best estimated value for the vertical shift of the curve in order to obtain absolute height values. Fig. 7c and d show that the corrected curves (dashed blue lines) agree well with the stage data (green squares).

The large number of stage stations in the Everglades also allows us to advance our space-based observations from relative to absolute measurements, by integrating both observation types. Analysis of the stage data reveals that the December (local dry season) data acquisition occurred at near-flat water surface conditions within each of the areas, despite about a one meter change between the areas (red squares in Fig. 7e and f). The flat December conditions are also supported by gate flow information (Table 2) indicating negligible water flow across the conservation areas. By using the December stage data as a reference level, we can calculate the June and August water levels (Fig. 7g and h). Our sample profiles (blue lines in Fig. 7e and f) agree well with available stage data for the two time periods.

The InSAR observations represent snapshots of dynamic water topography during the June and August observations, dominated by gate operations (Table 2, Fig. 7), allowing water to flow from area 1 to 2A and from 2A to 2B. Using the gate flow information, the following details can be observed and explained, illustrative of how InSAR data in wetlands provides fine

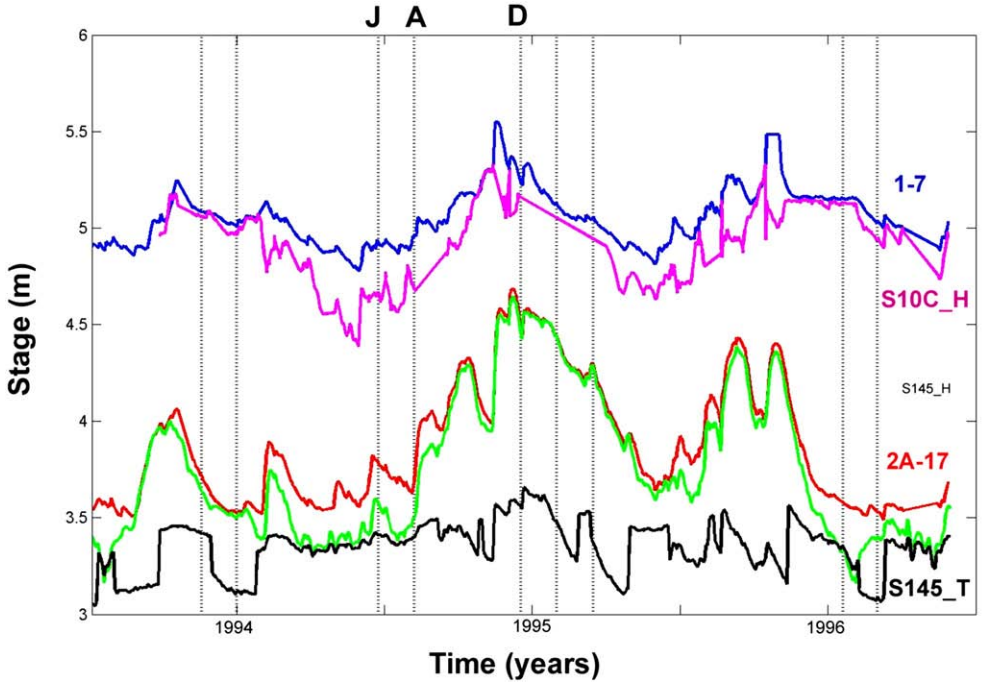

Fig. 8. Daily average water level time series collected at 5 stage station in areas 1, 2A, and 2B, along the profile shown in Fig. 5 (data source DBHYDRO). The vertical dotted lines mark the JERS-1 acquisition dates. The series show abrupt water level variations due to gate operation and rainfall, suggesting that the InSAR-detected water level changes represent the difference between two stage levels and cannot be used to determine rate of change. J, A, and D denotes the June, August and December acquisition dates used for the WCAs analysis (Figs. 6 and 7).

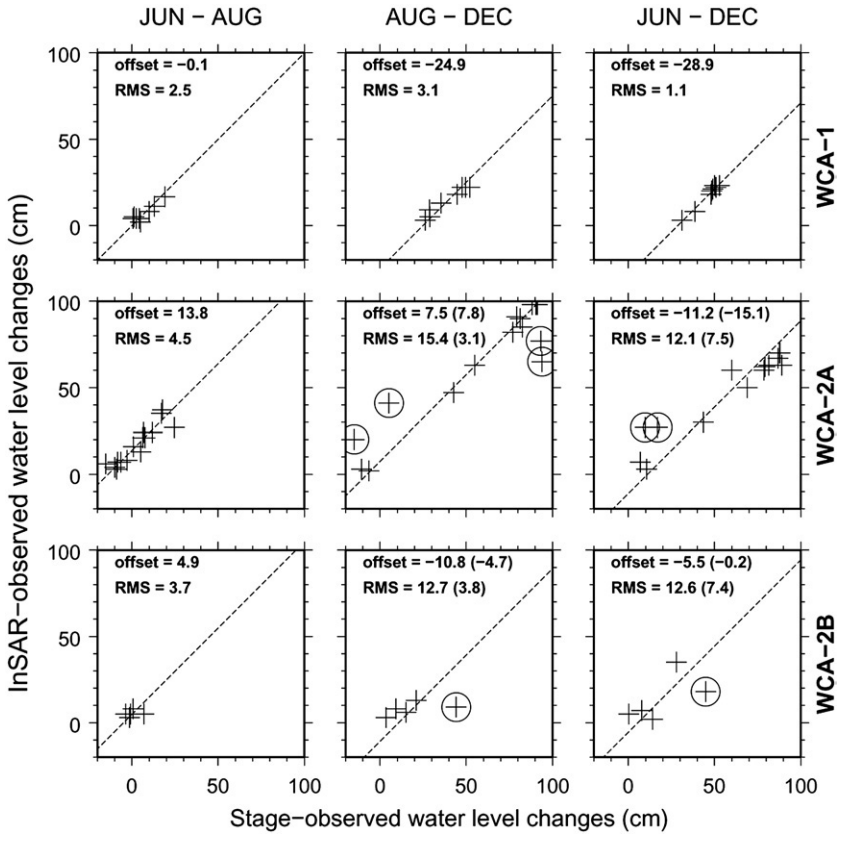

Fig. 9. Comparison between the zero-offset InSAR and the stage data calculated separately for each area in each interferogram. The bracket values are obtained after removing outliers (marked by circles).

Table 2
Flow observation (CFS — cubic feet per second; cubic meter per second values are given in the brackets) collected by the SFWMD during the JERS data acquisition at the gates feeding and draining area 2A

Station	Levee	Symbol	1994/06/26	1994/08/09	1994/12/19
S10D	1-2A	D	0	1170 (33.1)	0
S10C	1-2A	C	489 (13.8)	1447 (41.0)	88 (2.5)
S10A	1-2A	A	510 (14.4)	1485 (42.1)	0
S144	2A-2B	4	90 (2.5)	83 (2.4)	0
S145	2A-2B	5	117 (3.3)	95 (2.7)	0
S146	2A-2B	6	82 (2.3)	53 (1.5)	0

(Data source: DBHYDRO). The symbol indicates the gate location in Fig. 7a.

detail for a variety of studies, e.g., in this case for assessment of gate operations to better mimic natural flow conditions for wetland restoration: (i) The observed difference across area 2A is significantly higher in August than June because of August's higher flow rate across the S-10 gates. (ii) The shape of the lowest water level change along the 1-2A levee is long and linear in August (Fig. 7b) and shorter in June because gate S-10D was closed during the June observation period. This difference in the S-10D flow rate between June and August also yields a radial flow pattern in the June–August interferogram (Fig. 7a). (iii) Both maps show three small bull's eye patterns in the north of area 2B, reflecting low flow rates across culverts 145, 146 and 147. (iv) The "bull's eye" patterns are not observed in the June–August interferogram (Fig. 7a), reflecting the existence of similar dynamic topography both in June and August caused by similar flow rates across the same gates.

5.2. Surface changes in the natural flow wetlands

Unlike the organized fringe pattern in the WCAs, the fringes in the natural flow environment (ENP and BC) are irregular and broad (Fig. 3). The natural flow areas are also characterized by a low fringe rate, reflecting low gradients of water level changes. In three out of the four western track interferograms (Fig. 3e, g, and h), the fringe rate is very low, 1–2 fringes spanning a length of more than 100 km. Only in the AUG–DEC interferogram (Figs. 3f and 4) the fringe is rate higher, but not as high as in the WCAs. The higher fringe rate in the AUG–DEC interferogram also display some small-scale structures (Fig. 4).

Three of the four western track interferograms show two longer wavelength features in the natural flow areas (Fig. 3e, f,

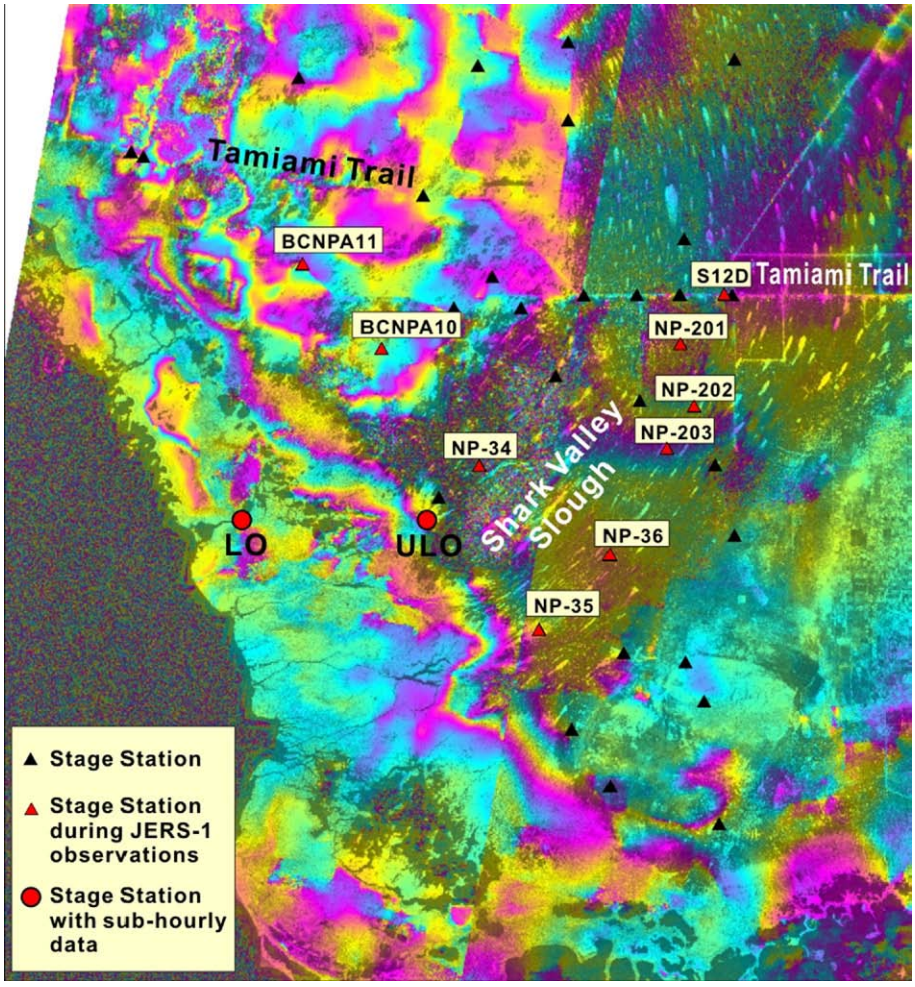

Fig. 10. AUG–DEC 1994 interferogram (lower left section of Fig. 7) showing water level changes in the BCNP and ENP, overlaid with stage station locations operated in 1994. Stations marked by red triangles show the location of the stations used in Fig. 11 and Table 3. Red circles mark the location of two stage stations with sub-hourly data shown in Fig. 12. The stations are: LO — Lostmans River and ULO — Upstream Lostmans River.

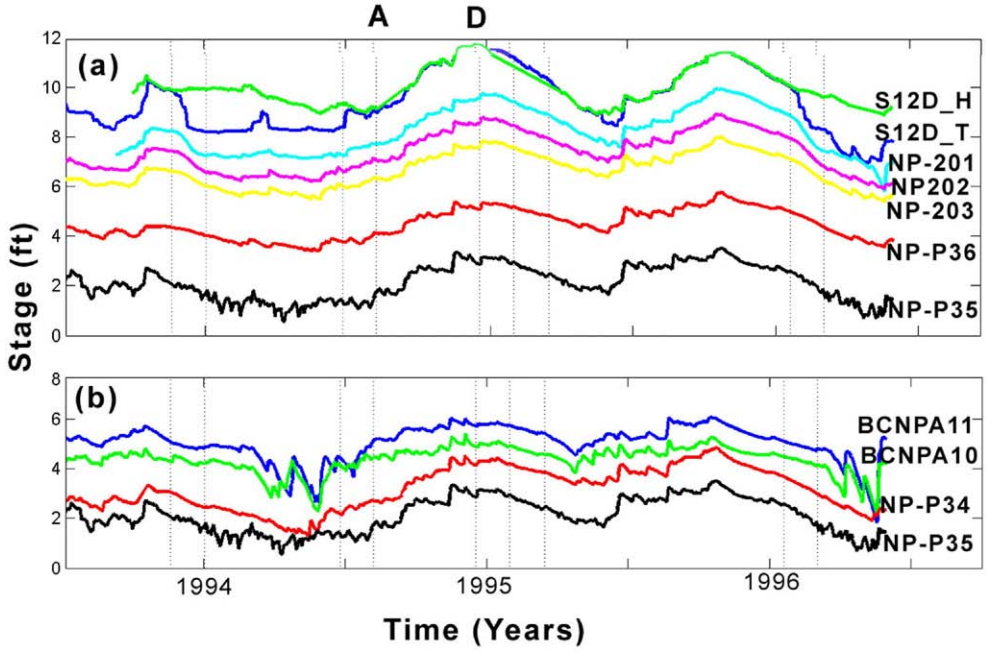

Fig. 11. Daily average water level time series collected at 9 stage station in The ENP and BCNP along Shark Valley Slough (a) and perpendicular to the Slough (b) (data source DBHYDRO). The vertical dotted lines mark the JERS-1 acquisition dates. The series show abrupt water level variations at station S12D_T, which is caused due to gate operation. Other stations show mostly seasonal variations but also some shorter term variations due to managed flow and rainfall events. A, and D denotes the August and December acquisition dates used for the mosaic interferogram (Figs. 4 and 10) and Table 3.

and h). The first is a prominent linear NW–SE fringe, subparallel to the coastline in the ENP. The second includes two parabolic-shape fringes, located south of the Tamiami Trail and oriented southwestward along the direction of the Shark Valley Slough are seen in Fig. 10. Available stage data from the acquisition period (1994–1996) allow us to study only the dual fringe south of the Tamiami Trail.

The three year stage time series in the natural flow area show a strong seasonal pattern in all sites but also shorter term variations caused by gate operation and rainfall (Fig. 11). The main source of water to the ENP is controlled supply from WCA-3A, north of the Tamiami Trail. The water is released to the EPN mainly through Shark Valley Slough via several gates according to a pre-defined protocol. Throughout most of the year, the gates are open, as shown by the same stage level in stations S12D_H and S12D_T, located north and south of the S12D gate, respectively (Fig. 11a). However, during some dry seasons, the gates are closed to maintain higher water levels in WCA-3A, which serves as water reservoir to the Miami–Fort Lauderdale metropolitan area. The gate operation affects stage levels of all the stations south of the gates with a very short delay (Fig. 11a). Although annual variations (Δh) in each station may reach one meter, the differential change between stations ($\Delta h_{ij} = \Delta h_i - \Delta h_j$) is very small. These small lateral water level changes can explain the lack of fringes in some of the interferograms over wide areas in the ENP and BCNP (Fig. 3e, g, and h). The two fringes that appear in the northern part of the Shark Valley Slough reflect delay in the flow pulses, mainly due to the flow resistance

Table 3
Comparison between stage and InSAR derived water level changes in the ENP and BCNP

Station	1994-8-9(10) ft (m)	1994-12-19(20) ft (m)	Diff (D-A) (cm)	w/r NP-P36 (cm)	InSAR [a] (cm)	Diff (cm)
S12C_T	8.95 (2.72)	11.62 (3.54)	81.4	51.2	54.2±5	−3.0±5
NP-201	7.69 (2.34)	9.55 (2.91)	56.7	26.5	33.1±5	−6.6±5
NP-202	7.04 (2.15)	8.55 (2.61)	46.0	15.8	18.2±5	−2.4±5
NP-203	6.32 (1.93)	7.58 (2.31)	38.4	8.2	10.6±5	−2.3±5
NP-P36	4.09 (1.25)	5.08 (1.55)	30.2	0	0	0.0
NP-P35	1.77 (0.54)	2.85 (0.87)	33.0	2.8	−0.5±5	3.2±5
NP-P34	2.69 (0.82)	4.31 (1.31)	49.4	19.2	–	–
BCNPA11	5.16 (1.57)	5.7 (1.74)	16.5	−13.7	−17.1±5	3.4±5
BCNPA10	4.46 (1.35)	4.87 (1.48)	12.5	−17.7	−23.3±5	5.6±5

InSAR observations are of the mosaic interferogram (Fig. 4) showing changes between 1994-8-9 and 1994-12-19 in the eastern track and 1994-8-10 and 1994-12-20 in the western track. Station locations are shown in Fig. 10. The 5 cm InSAR uncertainty level was derived from our analysis in the WCAs.
– Not available measurements due to low coherence.
[a] Water level change estimated from western JERS-1 track (eastern JERS-1 track).

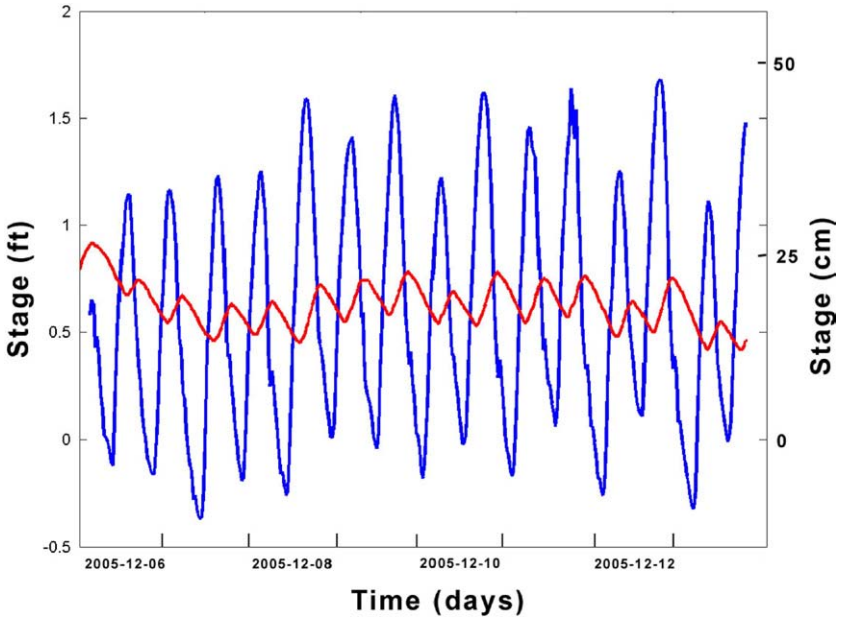

Fig. 12. Eight day-long sub-hourly water level time series collected at the Lostmans River (blue) and Upstream Lostmans River (red). The two stations are located in the salt-water mangrove wetland and are affected by ocean tides (station locations are shown in Fig. 10). The near shore station (blue) shows significantly higher daily variations (25–35 cm amplitude) with respect to the inland stations (red — 3–5 cm amplitude). (Data source: USGS real-time national water resources).

through the wetland vegetation. The observed InSAR water level variations are consistent with the stage data within a few cm, the approximate uncertainty level (Table 3). The time series of stations located normal to the direction of the Shark Valley Slough show larger lateral variations between stations (Fig. 11b), suggesting higher sensitivity of InSAR observations for detecting flow features directed normal to the overall flow direction.

The most noticeable feature in the natural flow area is the elongated fringe oriented NW–SE, sub-parallel to the western coast line (Figs. 3 and 4). Unfortunately, there are no archived stage data southwest of this feature that can be used to study these observed water level changes (Fig. 10). Nevertheless, using additional knowledge and more recent stage observations from this area, we can explain the nature of these observed elongated fringes. The first clue for understanding the nature of these elongated fringes is their consistent location along the eastern edge of the mangrove marsh right at the transition between saltwater (mangrove) and fresh water (woody — BCNP, and herbaceous — Shark Valley Slough) wetlands. The second clue is derived from field observations, indicating significant daily water level variations in the mangrove area due to ocean tides. Combining these two observations, we suggest that the elongated fringes along the vegetation transition reflect daily water level changes across the saltwater marsh due to ocean tides. Recent tide data (December, 2005) from two stage stations in the mangrove area (Fig. 10) with sub-hourly time series show significant daily water level variations due to ocean tide (Fig. 12). Furthermore, the two time series show that the near shore station (blue) has higher daily variations (25–35 cm) with respect to the inland stations (red — 3–5 cm). Because the interferogram shows water level changes between two acquisitions obtained during two different ocean tide levels, the changes in the mangrove wetland mainly show tide variations. One exception (Fig. 3g) shows no elongated NW–SE fringe. This pair was acquired over a time span of 308 days, at most likely very similar tide conditions.

6. Discussion

Our InSAR results show that L-band SAR data is very useful for detecting water level changes in most investigated wetland types. The coherence level and, hence, quality of InSAR observations depends on the scattering environment and the interferogram's time span. Highest coherence levels are obtained in the urban and woody wetland environments (Table 1). Over herbaceous wetland vegetation, the coherence level is higher for the one-repeat orbit cycle (44 days) and degrades as the interferogram time span increases. The first wetland type that looses phase is the herbaceous (sawgrass) wetland with time span greater than six months (Fig. 3d). However, woody wetlands can maintain phase for more than a year (e.g., WCA-1 in Fig. 3d) and in some cases over more than three years (Lu et al., 2005). The result that interferometric phase is maintained over both woody and herbaceous vegetations suggest that double-bounce is the dominant backscatter mechanism in both wetland environments.

The interferograms provide accurate measure of vertical movement of changes in the wetland water surface every repeat cycle of the JERS-1 satellite (44 days), or its multiples. However, in a single case we were able also to detect changes occurring within one day. This special case is the mosaic interferogram (Fig. 4), which juxtapose two interferograms separated by almost exactly 24 hours. The mosaic interferogram was concatenated by matching phase both in the northern and southern section of the study area, showing no offset along those parts of

the suture. However, in the central part of the Everglades there are small offsets along the suture, suggesting changes in the water level of up to quarter a cycle (4 cm) within a single day.

Previous InSAR studies of wetlands (Alsdorf et al., 2001, 2000) used the observed values to determine rate of change of water level between acquisitions assuming uniform change with time (dh/dt). This assumption is reasonable for the open Amazon Basin interferograms, with short time spans between acquisitions (less than 44 days). However, it is meaningless in the highly managed Everglades environment and especially with our 44–396 days time span. Stage (water level) time series of several stations in the study area show abrupt changes in water levels due to gate operations, as well as high variability between nearby stations over a few days (Fig. 8). In this case, the average rate of change between the acquisition dates is not very meaningful. A better and simpler way to interpret the observations is to consider them simply as lateral water level difference between two acquisitions ($\Delta h = h_2 - h_1$). In other words, the observations represent a difference between two states of water levels (snapshots). More importantly, knowledge of either h_2 or h_1 will then enable estimation of absolute height at the other time. In summary, the time span between acquisitions plays an important role in the interferometric coherence and its ability to maintain phase, but not in the way we interpret the observations.

Although our study was limited to south Florida wetlands, it has important implications for other large-scale wetland regions worldwide. South Florida has a variety of wetland vegetation, including woody, herbaceous, mangrove and prairie, as well as managed and natural flow areas. In addition, these wetlands are monitored by a dense network of over 200 ground-based stage stations, which is probably the densest network in the world. In light of the variable environment and the dense stage network, south Florida can be viewed as a large-scale laboratory for testing space-based technologies for hydrological applications (Wdowinski et al., 2005). Our results show very different fringe patterns in the managed and the natural flow areas. In the managed areas, the fringes are well organized and often truncated by managed water control structures. Although this managed environment is not representative of most wetlands, the large surface level changes detected there (up to 7 cycles ~1 m) allowed us to quantify the accuracy of the wetland InSAR method. The irregular fringe pattern observed in the natural flow areas is more representative of other large-scale wetlands. Our results suggest that water levels increase or decrease in most of the wetland area at a similar rate. Only after a significant rainfall event or after a large upstream flow influx, we should expect to detect changes reflecting laterally differential changes in water levels.

This study is based on archived L-band data that were acquired over south Florida during the years 1993–1996 by the JERS-1 satellite, which operated during the period 1992–1998. For most of the subsequent decade, no civilian L-band SAR satellite was in orbit. In January 2006 the Japanese's Advanced Land Observing Satellite (ALOS) was launched. After almost a year of successful calibration and validation, the satellite started acquiring data in December 2006, mostly according to a global acquisition plan. This plan was prepared several years ago, with an emphasis on global mapping of tropical and boreal forests, as a tool for monitoring the Kyoto accord (Rosenqvist et al., 2003). As a result, the number of planned acquisitions over wetlands is limited. For example, south Florida will be covered by nine cycles during a three year time period (2007–2009), with 44–180 days time span between acquisitions. Although this planned coverage is sufficient to maintain phase between most acquisitions, it would be beneficial to increase the number of acquisitions over wetland areas, as wetland surface flow and water levels can change rapidly within days. Furthermore, pre-mission planning of high temporal coverage over wetlands will be very useful in future L-band SAR missions.

Wetland InSAR applications include water level monitoring with high spatial resolution, detection of flow patterns and flow discontinuities, and constraining high resolution flow models (Wdowinski et al., 2006). Although here we focused mainly on the L-band InSAR observations and not on the applications, our observations can be used to constrain wetland flow models. Wdowinski et al. (2004a) used a subset of this data (three interferograms of the eastern track from second half of 1994) to constrain a one-dimensional diffusion flow model. Based on the space-based observations, they estimated flow diffusivity for the Everglades, as 23–91 m^2/s, which is similar to the diffusivity values estimated by Bolster and Saiers (2002) but is significantly lower than the 250 m^2/s often used in regional models (Lal, 2000). One of the interferograms described here (Fig. 3h) have been used to constrain the Tidal and Inflow in the Marshes of the Everglades (TIME) model (Swain et al., 2004). The TIME model investigates interacting effects of freshwater inflows and coastal driving forces (tides) in and along the mangrove ecotone of the Everglades National Park. The model was calibrated for the 1996–2002 time period, because reliable field observations are available for that time period. Unfortunately most of the JERS-1 data were acquired over south Florida prior to 1996. Only the two latest acquisitions of the eastern track (Figs. 2, 3h) can be used to constrain the TIME model. A comparison between the L-band interferogram and water level computed by the model show similarities in the long wavelength water level distribution, but some significant changes in short wavelength structures (Kim et al., 2006). The other L-band interferograms presented here (Fig. 3) can be used in the future to constrain other flow models that are currently developed by the SFWMD and the USGS for the entire Everglades watershed (e.g., Jones, 2006).

7. Conclusions

Interferometric analysis of twelve JERS-1 SAR passes acquired over south Florida during the years 1993–1996 show that L-band interferograms are very useful for detecting wetland water level changes. Although our study is limited to south Florida it has implication to many large-scale wetlands, because south Florida wetlands are very diverse, consisting of woody, herbaceous, prairie, and salt-water mangrove, as well as managed and natural flow environments. Furthermore a dense stage monitoring network provides sufficient ground truthing data needed for verification and calibration of the space-based

observations. We conducted a coherence analysis of the various wetland environments, which yielded high coherence values in woody wetlands (0.42), intermediate values in the saltwater mangrove and prairie wetlands (0.30–0.32), and low values in the herbaceous wetlands (0.27). These coherence levels, which were calculated from interferograms with 44-day time span (one repeat orbit), degrades in interferograms with larger time span. We found that interferograms with time span less than six months support phase observations in all wetland environments. Interferograms spanning over longer time span maintain phase over woody wetlands, but not over herbaceous ones.

Obtaining phase throughout south Florida allows us to characterize water level changes in the different wetland environments. The most noticeable changes occur between the managed and naturally flowing wetlands. In the managed wetland environment, fringes are organized, follow some of the water management structures in place, and have high fringe-rate. In naturally flowing areas, the fringes are irregular and have a low fringe-rate. Using stage data from the managed wetland area, we were able to quantify the accuracy of the InSAR measurements in the range of 5–10 cm. The stage data also allowed us to translate the observed water level changes into absolute water levels, reflecting dynamic water topography in response to hydraulic structure operations, such as gate opening. InSAR observations in the naturally flowing areas show a lower level of water level changes due to the larger extent of uninterrupted flow. Larger scale features in these areas include flow along the Shark Valley Slough and daily water level changes due to ocean tides in the fringing mangrove marsh.

Acknowledgements

We acknowledge the support and collaboration of the Department of the Interior, U.S. Geological Survey and the Florida Water Resources Research Center, University of Florida, under Grant No. 04HQGR0160, as well as, NASA and ONR. The work of S-W Kim was funded by the Korea Research Foundation Grant funded by Korea Government (MOEHRD, Basic Research Promotion Fund: No. M01-2004-000-20345-0). We thank Matt Pritchard for his help with the ROI_PAC software, Virginia Walsh for access to the Miami–Dade's WASD wellfield data, JAXA for access to the JERS data, SFWMD and USGS for access to stage data, Mike Waldon and Laura Brandt for the airboat field trip in A.R.M. Loxahatchee National Wildlife Refuge, and three anonymous reviewers. This is CSTARS contribution #13.

References

Alsdorf, D., Birkett, C., Dunne, T., Melack, J., & Hess, L. (2001). Water level changes in a large Amazon lake measured with spaceborne radar interferometry and altimetry. *Geophysical Research Letters*, *28*, 2671−2674.

Alsdorf, D. E., Melack, J. M., Dunne, T., Mertes, L. A. K., Hess, L. L., & Smith, L. C. (2000). Interferometric radar measurements of water level changes on the Amazon flood plain. *Nature*, *404*, 174−177.

Amelung, F., Galloway, D. L., Bell, J. W., Zebker, H. A., & Laczniak, R. J. (1999). Sensing the ups and downs of Las Vegas: InSAR reveals structural control of land subsidence and aquifer-system deformation. *Geology*, *27*, 483−486.

Baer, G., Schattner, U., Wachs, D., Sandwell, D., Wdowinski, S., & Frydman, S. (2002). The lowest place on Earth is subsiding — an InSAR (interferometric synthetic aperture radar) perspective. *Geological Society of America Bulletin*, *114*, 12−23.

Bawden, G. W., Thatcher, W., Stein, R. S., Hudnut, K. W., & Peltzer, G. (2001). Tectonic contraction across Los Angeles after removal of groundwater pumping effects. *Nature*, *412*, 812−815.

Bolster, C. H., & Saiers, J. E. (2002). Development and evaluation of a mathematical model for surface-water flow within the Shark River Slough of the Florida Everglades. *Journal of Hydrology*, *259*, 221−235.

Bourgeau-Chavez, L. L., Smith, K. B., Brunzell, S. M., Kasischke, E. S., Romanowicz, E. A., & Richardson, C. J. (2005). Remote monitoring of regional inundation patterns and hydroperiod in the greater everglades using synthetic aperture radar. *Wetlands*, *25*, 176−191.

Buckley, S. M., Rosen, P. A., Hensley, S., & Tapley, B. D. (2003). Land subsidence in Houston, Texas, measured by radar interferometry and constrained by extensometers. *Journal of Geophysical Research—Solid Earth*, *108*.

Buckley, S., Rossen, P., & Persaud, P. (2000). *ROI_PAC Documentation — Repeat Orbit Interferometry Package.*

Burgmann, R., Rosen, P. A., & Fielding, E. J. (2000). Synthetic aperture radar interferometry to measure Earth's surface topography and its deformation. *Annual Review of Earth and Planetary Sciences*, *28*, 169−209.

Colesanti, C., & Wasowski, J. (2006). Investigating landslides with space-borne synthetic aperture radar (SAR) interferometry. *Engineering Geology*, *88*, 173−199.

Dai, F. C., Lee, C. F., & Ngai, Y. Y. (2002). Landslide risk assessment and management: an overview. *Engineering Geology*, *64*, 65−87.

Douglas, M. S. (1947). *Everglades: River of Grass.* New York: Rinehart.

Goldstein, R. M., Engelhardt, H., Kamb, B., & Frolich, R. M. (1993). Satellite radar interferometry for monitoring ice-sheet motion — Application to an Antarctic Ice Stream. *Science*, *262*, 1525−1530.

Goldstein, R. M., & Werner, C. L. (1998). Radar interferogram filtering for geophysical applications. *Geophysical Research Letters*, *25*(21), 4035−4038.

Hanssen, R. (2001). *Radar interferometry.* Dordrecht: Kluwer Academic Publishers.

Jones, J. W. (2006). *Everglades Depth Estimation Network (EDEN) Digital Elevation Model Research and Development, Greater Everglades Ecosystem Restoration (GEER) Conference: Orlando, FL* (pp. 112). Abstract volume.

Kasischke, E. S., & Bourgeau-Chavez, L. L. (1997). Monitoring South Florida wetlands using ERS-1 SAR imagery. *Photogrammetric Engineering and Remote Sensing*, *63*, 281−291.

Kasischke, E. S., Smith, K. B., Bourgeau-Chavez, L. L., Romanowicz, E. A., Brunzell, S., & Richardson, C. J. (2003). Effects of seasonal hydrologic patterns in south Florida wetlands on radar backscatter measured from ERS-2 SAR imagery. *Remote Sensing of Environment*, *88*, 423−441.

Kim, S. -W., Wdowinski, S., Amelung, F., & Dixon, T. H. (2005). *C-band interferometric SAR measurements of water level change in the wetlands: examples from Florida and Louisiana, IGARSS 05: Seoul, Korea* (pp. 2708−2710).

Kim, S. -W., Wdowinski, S., Dixon, T., & Amelung, F. (2006). *SAR Interferometric Coherence Analysis of Wetlands in South Florida: Greater Everglades Ecosystem Restoration (GEER) Conference* (pp. 119). Abstract Volume.

Kimura, H., & Yamaguchi, Y. (2000). Detection of landslide areas using satellite radar interferometry. *Photogrammetric Engineering and Remote Sensing*, *66*, 337−344.

Lal, A. M. W. (2000). Numerical errors in groundwater and overland flow models. *Water Resources Research*, *36*, 1237−1247.

Lin, S., & Gregg, R. (1988). *Water budget analysis: Water Conservation Area*, *vol. 1*. (pp.)West Palm Beach, FL: South Florida Water Management District.

Lu, Z., Crane, M., Kwoun, O. I., Wells, C., Swarzenski, C., & Rykhus, R. (2005). C-band radar observes water level change in swamp forests. *Eos, Transactions of the American Geophysical Union*, *86*, 141−144.

Massonnet, D., & Feigl, K. L. (1998). Radar interferometry and its application to changes in the Earth's surface. *Reviews of Geophysics*, *36*, 441−500.

Massonnet, D., Rossi, M., Carmona, C., Adragna, F., Peltzer, G., Feigl, K., et al. (1993). The displacement field of the Landers earthquake mapped by radar interferometry. *Nature*, *364*, 138−142.

Mohr, J. J., Reeh, N., & Madsen, S. N. (1998). Three-dimensional glacial flow and surface elevation measured with radar interferometry. *Nature*, *391*, 273−276.

Raucoules, D., Maisons, C., Camec, C., Le Mouelic, S., King, C., & Hosford, S. (2003). Monitoring of slow ground deformation by ERS radar interferometry on the Vauvert salt mine (France) — Comparison with ground-based measurement. *Remote Sensing of Environment*, *88*, 468−478.

Richards, J. A., Woodgate, P. W., & Skidmore, A. K. (1987). An explanation of enhanced radar backscattering from flooded forests. *International Journal of Remote Sensing*, *8*, 1093−1100.

Rosen, P. A., Hensley, S., Zebker, H. A., Webb, F. H., & Fielding, E. J. (1996). Surface deformation and coherence measurements of Kilauea volcano, Hawaii, from SIR-C radar interferometry. *Journal of Geophysical Research-Planets*, *101*, 23109−23125.

Rosenqvist, A., Milne, A., Lucas, R., Imhoff, M., & Dobson, C. (2003). A review of remote sensing technology in support of the Kyoto Protocol. *Environmental Science & Policy*, *6*, 441−455.

Shimada, M. (2002). *User's guide to NASDA's SAR products Ver.3: Tokyo, Japan.*

Sklar, F. H., Van Der Valk, A., & Valk, A. V. D. (2003). *Tree islands of the Everglades.* Dordrecht: Kluwer Academic Publishers.

Swain, E. D., Wolfert, M. A., Bales, J. D., & Goodwin, C. R. (2004). Two-Dimensional Hydrodynamic Simulation of Surface-Water Flow and Transport to Florida Bay through the Southern Inland and Coastal Systems (SICS). *Water-Resources Investigations Report, USGS* (pp. 69).

Tesauro, M., Berardino, P., Lanari, R., Sansosti, E., Fornaro, G., & Franceschetti, G. (2000). Urban subsidence inside the city of Napoli (Italy) observed by satellite radar interferometry. *Geophysical Research Letters*, *27*, 1961−1964.

Wdowinski, S., Amelung, F., Miralles-Wilhelm, F., Dixon, T. H., & Carande, R. (2004a). Space-based measurements of sheet-flow characteristics in the Everglades wetland, Florida. *Geophysical Research Letters*, *31*.

Wdowinski, S., Amelung, F., & Dixon, T. (2004b). Towards operational monitoring of wetland water levels using InSAR: Applications for the Everglades Restoration Project.*Eos, Transactions of the American Geophysical Union*, *85*(47) Fall Meet. Suppl., Abstract C21B-05.

Wdowinski, S., Amelung, F., Dixon, T., Kim, S., Osmanoglu, B., Kartal, M., et al. (2005). The Everglades wetlands as a laboratory for testing and calibrating space-geodetic hydrological technologies.*Eos, Transactions of the American Geophysical Union*, *86* p. Spring Meet. Suppl., Abstract G23A-04.

Wdowinski, S., Kim, S., Amelung, F., & Dixon, T. (2006). Wetland InSAR: A new space-based hydrological monitoring tool of wetlands surface water level changes. *GlobWetland Symposium Proceedings: Frescati, Itali* (pp. 6).

Zebker, H. A., Rosen, P. A., & Hensley, S. (1997). Atmospheric effects in interferometric synthetic aperture radar surface deformation and topographic maps. *Journal of Geophysical Research—Solid Earth*, *102*, 7547−7563.